A Numerical Calculation of the Capacitance for the Rectangular Coaxial Line with Offset Inner Conductor Having an Anisotropic Dielectric

HISASHI SHIBATA, SHINYA MINAKAWA, AND RYUITI TERAKADO

Abstract—**The capacitances of the rectangular coaxial lines with an offset zero-thickness inner conductor having a sapphire dielectric are presented by using an expanded charge simulation method. In order to apply the method to an anisotropic region, we propose an electric potential formula for a two-dimensional system consisting of a line charge and an infinite plate conductor which are arbitrarily situated in the region. The potential formula is analytically derived by means of an affine transformation, a conformal mapping technique, and the method of images. The capacitance calculated using this method is in good agreement with those of other available methods.**

I. Introduction

THE RECTANGULAR coaxial line has been used in microwave circuits and EMI measurement systems [1]. The analysis of the structures with a zero-offset inner conductor has been presented by Magnus and Oberhettinger [2], Anderson [3], and Cohn [4]. Magnus and Oberhettinger have also given in [2] the characteristic impedance of the stripline with a circular outer conductor. Chen [5] has obtained the capacitances of the rectangular structures for the horizontally and vertically offset inner conductor of finite thickness. Tippet and Chang [6] have presented an interesting formula for the capacitance of the structure with an offset zero-thickness strip by using a singular-integral-equation technique. Riblet [7] has presented the even- and odd-mode characteristic impedances of the rectangular coaxial structure with off-centered strips by the Schwartz–Cristoffel transformation method. However, the medium between the outer and inner conductors in the above literatures was composed of isotropic dielectric.

The two-dimensional space between the two conductors of the rectangular coaxial line, which is discussed in this paper, is filled with an anisotropic medium. The cross section of the structure is shown in Fig. 1. The zero-thickness inner conductor is arbitrarily situated. The structure with the anisotropic medium can be transformed to one with a corresponding isotropic medium by means of a transform method [8]–[10] or the method by normalized metric factor [11]. By applying the transformation, which has been reported by Kusase and Terakado [10] and was used in [12] and [13] by Shibata *et al.*, however, the shapes of outer conductors in Fig. 1 are generally converted into parallelograms. Therefore, the formulas in the literature [2]–[7] cannot be applied to the analysis of the structure shown in Fig. 1, except for the extreme cases, i.e., $\theta = 0$ and $\pi/2$, and a numerical method is needed. The parameter θ is the angle between the principal axes of the anisotropic medium and the $x-y$ coordinates. There are various numerical methods [14] which are applicable to the isotropic region. However, it is advantageous if the method can be directly applicable to the anisotropic region [15], [16]. To obtain the capacitances accurately, however, these methods are not always convenient, because the distributed charges on the strip shown in Fig. 1 must be computed with the potential values at a large number of grid points of the neighborhood of the strip.

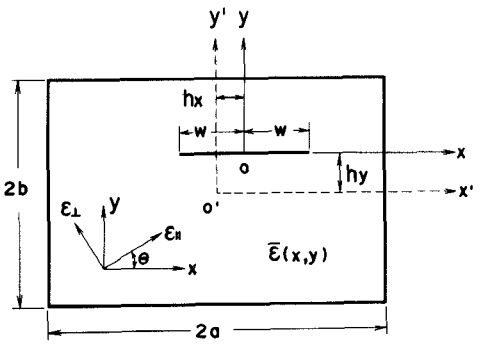

Fig. 1. Cross section of the rectangular coaxial line with offset inner conductor having an anisotropic medium. (Point O' is the center of the rectangular.)

In the present work, a charge simulation method [17], [18] is used to obtain the capacitance of the structure shown in Fig. 1. This method has a high accuracy if we use a good arrangement of the discrete charges, even though a small number of charges are used. To apply the method to the anisotropic region, we present the electrostatic field generated by a line charge and an infinite plate conductor which are located at any position in the region. An affine transformation, a conformal mapping technique, and the

Manuscript received July 6, 1982; revised December 17, 1982.

H. Shibata and S. Minakawa are with the Department of Electrical Engineering, Ibaraki Technical College, Katsuta, Ibaraki, 312, Japan.

R. Terakado is with the Department of Electrical Engineering, Faculty of Engineering, Ibaraki University, Hitachi, Ibaraki, 316, Japan.

0018-9480/83/0500-0385$01.00 ©1983 IEEE

method of images are used to obtain the potential function. We also present exact distributions of equipotentials and lines of electric flux in the region by using the function. Application to the charge simulation method of the potential function, which already satisfied the boundary condition on the strip conductor, yields the decrease in the number of charges by comparison with the conventional method [17]. This consideration has been reported for an isotropic region by Murashima [19]. The values of capacitances for both $\theta = 0$ and $\theta = \pi/2$ of the structures with offset and zero-offset strips shown in Fig. 1 are compared with those calculated by authors using other available methods [2], [6]. And so the capacitance obtained by the method of this paper will be shown to have a satisfactory accuracy.

The merit of this method is that it can be applied to the striplines using the anisotropic medium with the outer conductors of arbitrary shape. The application is exemplified with a circular outer conductor.

II. Potential Function in Anisotropic Region

Now consider the two-dimensional region which is filled with the anisotropic medium of the following permittivity tensor:

$$\bar{\epsilon}(x, y) = \epsilon_0 \begin{bmatrix} \epsilon_{\parallel}\cos^2\theta + \epsilon_{\perp}\sin^2\theta & (\epsilon_{\parallel} - \epsilon_{\perp})\sin\theta\cos\theta \\ (\epsilon_{\parallel} - \epsilon_{\perp})\sin\theta\cos\theta & \epsilon_{\perp}\cos^2\theta + \epsilon_{\parallel}\sin^2\theta \end{bmatrix} \tag{1}$$

for the $x-y$ coordinates as shown in Fig. 2(a). Where $\epsilon_{\parallel}$, $\epsilon_{\perp}$, and ϵ_0 are the principal axes-relative dielectric constants of the anisotropic medium and the permittivity of vacuum, respectively. We derive a potential function $\phi(x, y)$ at any point in the region including a plate conductor with width $2w$, and a line charge with magnitude λ per unit length. The function is a solution of Poisson's equation

$$\nabla\cdot\{\bar{\epsilon}(x, y)\cdot\nabla\phi(x, y)\} = -\lambda(x_0, y_0) \tag{2}$$

which satisfies the boundary condition on the plate conductor, i.e., $\phi = \phi_0$ (= const). First, in order to obtain the solution of (2) for the system shown in Fig. 2(a), we transform the anisotropic region (Z-plane) in Fig. 2(a), with the exception of the point of charge, into a corresponding isotropic region (W-plane) as shown in Fig. 2(b) by the following affine transformation [10], [12]:

$$\begin{bmatrix} u \\ v \end{bmatrix} = \begin{bmatrix} 1 & \beta \\ 0 & \alpha \end{bmatrix}\cdot\begin{bmatrix} x \\ y \end{bmatrix} \tag{3}$$

where

$$\alpha = \frac{\sqrt{\epsilon_{\perp}/\epsilon_{\parallel}}}{\sin^2\theta + (\epsilon_{\perp}/\epsilon_{\parallel})\cos^2\theta} \qquad \beta = \frac{(\epsilon_{\perp}/\epsilon_{\parallel} - 1)\sin\theta\cos\theta}{\sin^2\theta + (\epsilon_{\perp}/\epsilon_{\parallel})\cos^2\theta}.$$

By applying (3), the permittivity of the isotropic region becomes $\epsilon_0\sqrt{\epsilon_{\parallel}\epsilon_{\perp}}$. But the width of plate conductor is invariant. Secondly, we transform the region in Fig. 2(b) into the region (T-plane) shown in Fig. 2(c) by the following conformal mapping function [20]:

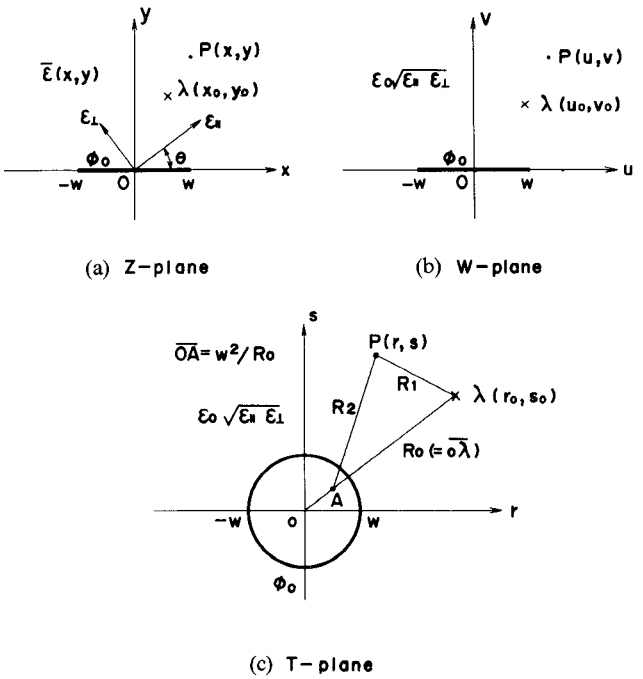

Fig. 2. Transformations to the isotropic regions from an anisotropic region and application of the method of images. (a) → (b): The affine transformation based on (3). (b) → (c): Conformal mapping based on (4).

$$W = \frac{1}{2}\left(T + \frac{w^2}{T}\right) \qquad W = u + iv \qquad T = r + is. \tag{4}$$

By this mapping, the region exterior to the plate is transformed into that exterior to the circle with radius w. Thus, the method of images is used to obtain the solution to the electrostatic problem involving a circular boundary. The position of the image of a line charge inside the circular conductor is a point A on a straight line which connects the point (r_0, s_0) to the origin O in the T-plane. The distance $\overline{OA}$ is w^2/R_0. The magnitude of the image charge is $-\lambda$. Then, the potential $\phi(r, s)$ at point P outside the circle is given by a line charge of magnitude λ at a point (r_0, s_0) and the image charge of magnitude $-\lambda$ at a point A as

$$\phi(r, s) = \phi_0 + \frac{\lambda}{2\pi\epsilon_0\sqrt{\epsilon_{\parallel}\epsilon_{\perp}}}\ln\frac{R_0R_2}{wR_1} \tag{5}$$

where R_1 and R_2 are the distances shown in Fig. 2(c). Finally, we obtain the potential function $\phi(x, y)$ at any point P in the Z-plane by substituting (3) and (4) in (5). That is

$$\phi(x, y) = \phi_0 + \frac{\lambda}{4\pi\epsilon_0\sqrt{\epsilon_{\parallel}\epsilon_{\perp}}}\ln F(x, y; x_0, y_0) \tag{6}$$

where

$$F(x, y; x_0, y_0) = \frac{\{f_1(x, y) - c_0 f_1(x_0, y_0)\}^2 + \{f_2(x, y) - c_0 f_2(x_0, y_0)\}^2}{c_0\left[\{f_1(x, y) - f_1(x_0, y_0)\}^2 + \{f_2(x, y) - f_2(x_0, y_0)\}^2\right]}$$

$$c_0 = w^2/4\left[\{f_1(x_0, y_0)\}^2 + \{f_2(x_0, y_0)\}^2\right] \qquad f_1(x, y) = \frac{x+\beta y}{1+g(x, y)} \qquad f_2(x, y) = \frac{\alpha y}{1-g(x, y)}$$

$$g(x, y) = w^2 \Bigg/ \left[\frac{\sqrt{(w+x+\beta y)^2+\alpha^2 y^2} + \sqrt{(w-x-\beta y)^2+\alpha^2 y^2}}{2} + \frac{\sqrt{(x+\beta y)^2+\alpha^2 y^2 - w^2 + \sqrt{\{w^2+(x+\beta y)^2+\alpha^2 y^2\}^2 - 4w^2(x+\beta y)^2}}}{\sqrt{2}} \right]^2.$$

Equation (6) gives the potential in the region exterior to the plate conductor. Of course, the potential on the conductor is ϕ_0. The electric field at any point in the Z-plane is derivable as the negative gradient of the potential (6). Equation (6) is also applicable to an isotropic region if we take $\epsilon_\perp/\epsilon_\parallel = 1$, i.e., $\alpha = 1$, $\beta = 0$.

In Fig. 3, we show the distributions of equipotentials and lines of electric flux in the region of Fig. 2(a) by using (6). Fig. 3(a) and (b) shows the field distributions with the parameters of $\epsilon_\perp/\epsilon_\parallel = 1/9$, $\theta = \pi/6$ (anisotropic), and $\epsilon_\perp/\epsilon_\parallel = 1$ (isotropic), respectively. To compare, the line charge and the plate conductor are placed on the same positions for both regions, respectively. Considerable differences of the properties of electric fields for the two regions are clearly presented in these figures. The curves in the Z-plane correspond to the following circle groups:

$$\left\{r - \frac{w^2 r_0(c-1)}{cw^2 - R_0^2}\right\}^2 + \left\{s - \frac{w^2 s_0(c-1)}{cw^2 - R_0^2}\right\}^2 = \left\{\frac{w\sqrt{c}\,(R_0^2 - w^2)}{cw^2 - R_0^2}\right\}^2,$$

$$c = \exp\left\{\frac{4\pi\epsilon_0\sqrt{\epsilon_\parallel\epsilon_\perp}\,(\phi - \phi_0)}{\lambda}\right\} \text{ for equipotential lines} \tag{7}$$

$$\left\{r - \frac{r_0 c(R_0^2 + w^2) - s_0(R_0^2 - w^2)}{2cR_0^2}\right\}^2 + \left\{s - \frac{s_0 c(R_0^2 + w^2) + r_0(R_0^2 - w^2)}{2cR_0^2}\right\}^2 = \left\{\frac{(R_0^2 - w^2)\sqrt{c^2+1}}{2cR_0}\right\}^2,$$

$$c = \tan\gamma \text{ for lines of electric flux}$$

in the T-plane. Plotted in Fig. 3(a) and (b) are the curves for the parameters with $4\pi\epsilon_0\sqrt{\epsilon_\parallel\epsilon_\perp}\,(\phi - \phi_0)/\lambda = 0.7m$ ($m = 0, 1, \cdots, 15$) and $\gamma = \pm\pi/2n$ ($n = 1, 2, \cdots, 5$).

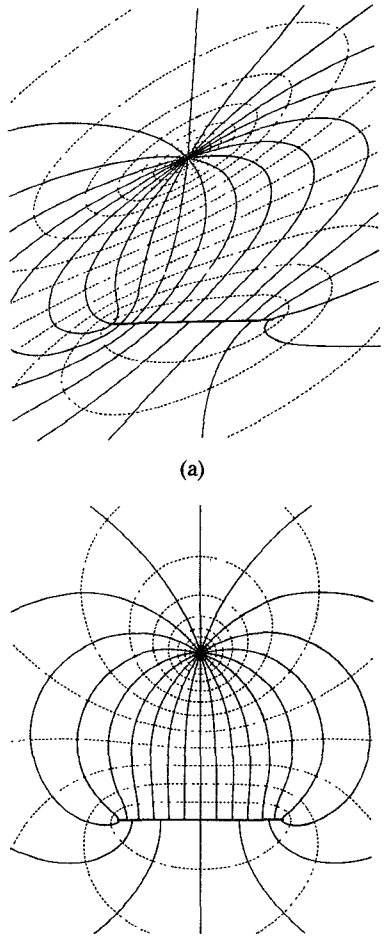

(a)

(b)

Fig. 3. Equipotentials and lines of electric flux ($w = 1$, $x_0 = 0$, $y_0 = 2$). (a) Anisotropic region ($\epsilon_\perp/\epsilon_\parallel = 1/9$, $\theta = \pi/6$). (b) Isotropic region ($\epsilon_\perp/\epsilon_\parallel = 1$). --------- Equipotential lines. —— Lines of electric flux.

If we need the potential function at any point for a conducting plate of width $2w$ charged with charge density λ per unit length, it can be readily obtained by using the function $g(x, y)$ in (6) as

$$\phi(x, y) = \phi_0 + \frac{\lambda}{4\pi\epsilon_0\sqrt{\epsilon_\parallel\epsilon_\perp}} \ln g(x, y). \tag{8}$$

Equation (8) corresponds to the electric fields by an infinite line charge λ on the origin in the T-plane. The

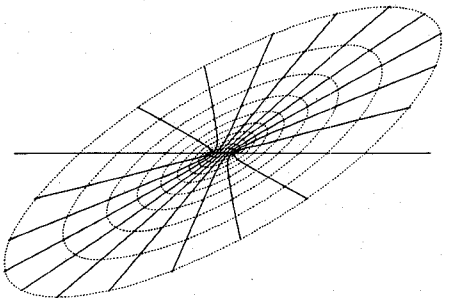

Fig. 4. Field distribution in anisotropic region ($\epsilon_\perp/\epsilon_\parallel = 1/9$, $\theta = \pi/6$) by a conducting plate. ---------- Equipotential lines. —— Lines of electric flux.

distributions of electric fields based on (8) are shown in Fig. 4 with parameters $\epsilon_\perp/\epsilon_\parallel = 1/9$ and $\theta = \pi/6$. The formula for the case of $\alpha = 1$, $\beta = 0$ is given in [21].

III. Application to Charge Simulation Method

In this section, we show that the potential function (6) can be applied to a charge simulation method [17], [18]. In the method, the distributed surface charges on the outer conductor are replaced by discrete fictitious line charges at infinity. Those charges are arranged outside of the conductor, as shown in Fig. 5.

Now we assume that the number of pairs of line charges and plate conductors is n. To determine the magnitude of these charges, n contour points are chosen on the outer conductor. By applying the superposition of the potential function (6) at every contour point, the system of n linear equations for n line charges is obtained as

$$\frac{1}{4\pi\epsilon_0\sqrt{\epsilon_\parallel\epsilon_\perp}}\left[\ln F(x_i, y_i; x_j, y_j)\right]\begin{bmatrix}\lambda_1\\ \vdots\\ \lambda_j\\ \vdots\\ \lambda_n\end{bmatrix} + n[\phi_0] = \begin{bmatrix}\phi_{c1}\\ \vdots\\ \phi_{ci}\\ \vdots\\ \phi_{cn}\end{bmatrix} \tag{9}$$

where ϕc_i $(i = 1, \cdots, n)$ are the potential values on the contour points. The pairs (x_i, y_i) and (x_j, y_j) are the coordinates of contour and of charge points, respectively. By solving the system of (9) under the boundary condition on the outer conductor, $\phi c_i = \phi c_0$ $(= \text{const})$, the magnitudes of those charges $[\lambda_j]$ are determined. So, the potential at a point (x, y) between the inner and outer conductors can be calculated analytically by superposition. That is

$$\phi(x, y) = n\phi_0 + \frac{1}{4\pi\epsilon_0\sqrt{\epsilon_\parallel\epsilon_\perp}}\sum_{j=1}^{n}\lambda_j \ln F(x, y; x_j, y_j). \tag{10}$$

By using (10), we can check whether the calculated charges are correct or not. The judgment is performed by comparing the potential at a number of check points located on the outer conductor with the given boundary potential. Of course the difference between those potentials must be lessened. The capacitance Ca per unit length is obtained as follows:

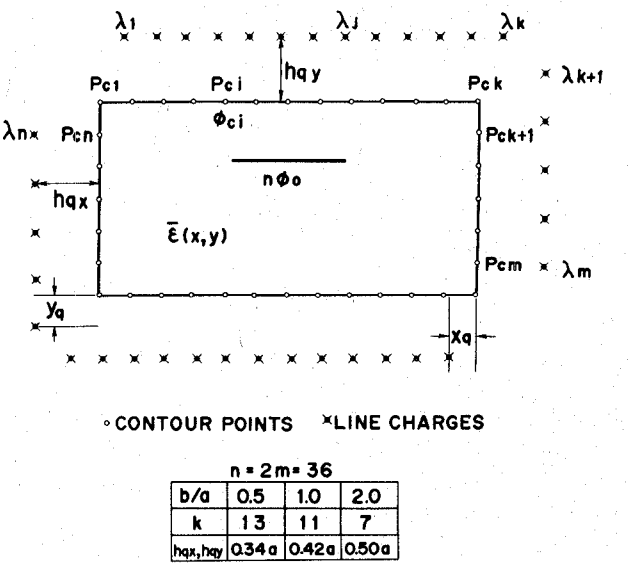

n = 2m = 36

b/a	0.5	1.0	2.0
k	13	11	7
hqx, hqy	0.34a	0.42a	0.50a

Fig. 5. Arrangement of line charges and contour points for the calculation of the field potential between outer and inner conductors by charge simulation method.

$$Ca = \left|\frac{1}{n\phi_0 - \phi_{c0}}\sum_{j=1}^{n}\lambda_j\right|. \tag{11}$$

The accuracy of (11) depends not only on the placement and the number of charges but also on the method of the system of equations in (9). For these problems, Murashima *et al.* [22], [23] discussed the properties of the potential error and the location as well as shape of the boundary. No discussion was presented, however, for a rectangular boundary.

The capacitance error of the structure shown in Fig. 1 calculated using (11) will be discussed in the following section.

IV. Numerical Evaluation of Capacitance

We calculate in this section the capacitances of the structure shown in Fig. 1 with a sapphire dielectric ($\epsilon_\parallel = 11.6$, $\epsilon_\perp = 9.4$) [24] by using the method presented in the previous section. The arrangement of the line charges and the contour points are shown in Fig. 5. In Fig. 5, we select the locations for the line charges and the contour points as follows.

a) The number of line charges n is chosen to be 36.
b) The contour points are equally placed on each side of rectangular.
c) The line charges are equally arranged on the straight lines which parallel the sides of the rectangular. The lengths of the straight lines equal to those of the respective sides.
d) The h_{qx} and h_{qy}, the distances between the straight lines and the sides, are chosen as shown in Fig. 5, respectively.
e) Moreover, the charges are horizontally slid for each

TABLE I
COMPARISON OF THE CAPACITANCES $Ca/\epsilon_0\sqrt{\epsilon_{\parallel}\epsilon_{\perp}}$ PER UNIT LENGTH FOR THE ZERO-OFFSET STRUCTURES WITH SAPPHIRE DIELECTRIC

hx=0.0 hy=0.0				
$\frac{b}{a}$	$\frac{w}{a}$	θ	$Ca/\epsilon_0\sqrt{\epsilon_{\parallel}\epsilon_{\perp}}$	
			Method B	Method A
0.5	0.1	0	2.37875	2.37875
		$\pi/2$	2.56979	2.56979
1.0	0.2	0	2.59301	2.59301
		$\pi/2$	2.70460	2.70460
2.0	0.6	0	4.63194	4.63198
		$\pi/2$	4.65335	4.65329

TABLE II
COMPARISON OF THE CAPACITANCES $Ca/\epsilon_0\sqrt{\epsilon_{\parallel}\epsilon_{\perp}}$ PER UNIT LENGTH FOR THE OFFSET STRUCTURES WITH SAPPHIRE DIELECTRIC

hx=0.0 θ=0.0				
$\frac{hy}{b}$	$\frac{b}{a}$	$\frac{w}{a}$	$Ca/\epsilon_0\sqrt{\epsilon_{\parallel}\epsilon_{\perp}}$	
			Method C	Method A
0.25	0.5	0.2	3.30091	3.31655
		0.6	6.66683	6.66888
	1.0	0.2	2.64439	2.64458
		0.6	5.00332	5.00345
	2.0	0.2	2.48804	2.48804
		0.6	4.64708	4.64665
0.50	0.5	0.2	3.71425	3.78599
		0.6	7.87796	7.88577
	1.0	0.2	2.86054	2.86346
		0.6	5.51966	5.52019
	2.0	0.2	2.53589	2.53593
		0.6	4.75462	4.75539

side of rectangular outer conductor. The distances x_q and y_q are

$$x_q = -\beta h_{qx}$$

and

$$y_q = -\frac{\beta}{\alpha^2+\beta^2} h_{qy}$$

respectively. By the slide, the potential errors on each side are averaged. Both x_q and y_q are zero when θ is either 0 or $\pi/2$.

We have to check the accuracy of this method based on the above locations. For the structure shown in Fig. 1, the analysis for the cases of arbitrary angle θ has not been presented. However, the capacitances for the cases of particular angles, i.e., $\theta = 0$ and $\pi/2$, can be obtained by bestowing the slight improvements in the conventional methods [2], [6]. Those methods will be shown presently in this section. Therefore, we first compare the values of capacitances using the method based on (11) with the analytical values for $\theta = 0$ and $\pi/2$.

The comparison of the capacitances of the rectangular coaxial lines is shown in Tables I and II. In Table I, the numerical results of $Ca/\epsilon_0\sqrt{\epsilon_{\parallel}\epsilon_{\perp}}$ of symmetrical lines by the method of this paper (method A) are compared with those calculated by authors using the conformal mapping method (method B) as

$$Ca = 4\epsilon_0\sqrt{\epsilon_{\parallel}\epsilon_{\perp}}\,\frac{K'(k)}{K(k)} \tag{12}$$

where

$$k = \mathrm{sn}\left\{\frac{w}{a}K(k_g), k_g\right\}$$

$$\frac{K'(k_g)}{K(k_g)} = \alpha\frac{b}{a} \qquad \alpha = \begin{cases} \sqrt{\epsilon_{\parallel}/\epsilon_{\perp}} & (\text{for } \theta = 0) \\ \sqrt{\epsilon_{\perp}/\epsilon_{\parallel}} & (\text{for } \theta = \pi/2) \end{cases}.$$

K and K' are complete elliptic integrals of the first kind. The formula for $\alpha = 1$ is given in [2]. Also in Table II, $Ca/\epsilon_0\sqrt{\epsilon_{\parallel}\epsilon_{\perp}}$ of the offset structure by method A is compared with those calculated by the improved formula of Tippet and Chang [6] (method C). We calculated the capacitances of method C by improving the coefficient as

$$A_1 = \frac{\cosh\frac{\alpha b\pi}{a} - \cosh\frac{\alpha h_y\pi}{a}}{\sinh\frac{\alpha b\pi}{a}} - 1$$

$$\alpha = \begin{cases} \sqrt{\epsilon_{\parallel}/\epsilon_{\perp}} & (\text{for } \theta = 0) \\ \sqrt{\epsilon_{\perp}/\epsilon_{\parallel}} & (\text{for } \theta = \pi/2) \end{cases} \tag{13}$$

and by substituting the coefficient for (24) in [6].

Comparing methods A and B, the capacitances of method A for the symmetrical structure obviously have a good accuracy. For the offset structure, the results of method A yield a small difference when compared to method C. Therefore, the capacitances calculated by the method of this paper seem to have satisfactory accuracy for the arbitrary angle θ. The capacitances $Ca/\epsilon_0\sqrt{\epsilon_{\parallel}\epsilon_{\perp}}$ per unit length versus the normalized width of the strip w/a for $b/a = 1$ are shown in Fig. 6. Plotted in Fig. 6 are design curves for zero offset and an offset ratio h_y/b of 0.5. Both curves are shown with the parameters θ of 0, $\pi/4$, and $\pi/2$, respectively. In Fig. 6, the values of capacitances for $w/a \gtrsim 0.8$ obtained by method A have an error. The arrangement of charges which was used to obtain the results of Fig. 6 is shown in Fig. 5. Also, the capacitance error based on the arrangement of charges shown in Fig. 5 gradually increases as the h_y increases from 0 to b. This fact indicates that the arrangement of charges shown in Fig. 5 is not all-powerful. Therefore, for $w/a \gtrsim 0.8$ and $h_y \to b$, the arrangement of charges must be changed. Moreover, we have to check over again whether the new arrangement of charges is correct or not. It is a disadvantage of this method, but the usefulness of this method sufficiently compensates for this weakness. The usefulness will be especially shown for the structures with arbitrary angles θ where the analytical solutions for the capacitance cannot be obtained. The practice is presented on the curves of both $h_y/b = 0$ and 0.5 with $\theta = \pi/4$ in Fig. 6 and the curves in Fig. 7. Fig. 7 shows $Ca/\epsilon_0\sqrt{\epsilon_{\parallel}\epsilon_{\perp}}$ versus θ for the structures with zero-offset strip. The slopes of the capacitances with θ increase as b/a decreases.

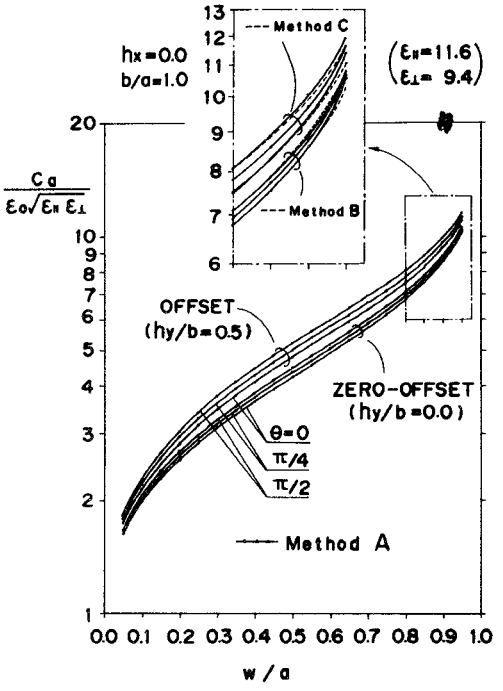

Fig. 6. Capacitances $Ca/\epsilon_0\sqrt{\epsilon_{\parallel}\epsilon_{\perp}}$ per unit length versus w/a for the rectangular coaxial lines with sapphire dielectric.

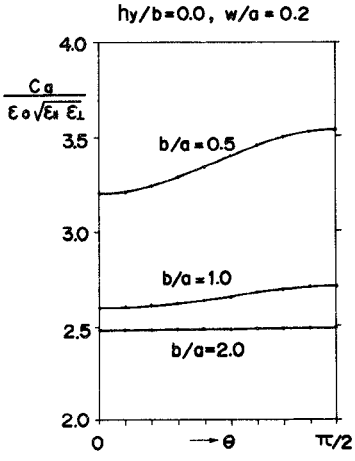

Fig. 7. Capacitances $Ca/\epsilon_0\sqrt{\epsilon_{\parallel}\epsilon_{\perp}}$ per unit length versus θ for the rectangular coaxial lines with sapphire dielectric.

Another considerable method to improve the accuracy of the capacitance is to augment the number of charges by comparison with one used in this paper. By the augmentation, the capacitance error is generally decreased, because the capacitance value theoretically approaches the true value if we use the arrangement of the discrete charges which has much the same effect as the true distribution of charge density on the outer conductor. However, we shall have to use great numbers of charges for the purpose.

A merit of the method of this paper is that it can be applied to the structures with arbitrary outer conductors. As an example, we present the application to the structure with a circular outer conductor as shown in Fig. 8. Table III shows the comparison of the capacitance C_0/ϵ_0 for the structure with zero-offset strip having the medium of $\epsilon_{\perp}/\epsilon_{\parallel} = 1$. The capacitances of method D in Table III are given

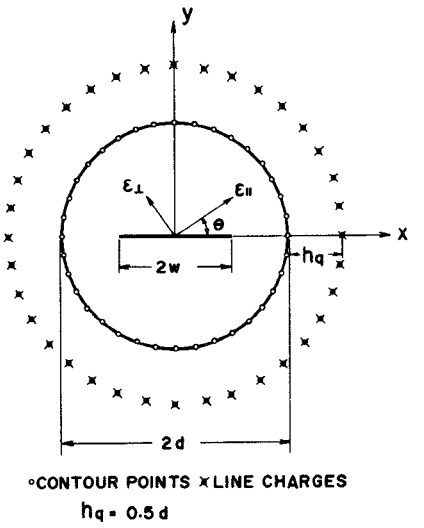

Fig. 8. Cross section of a coaxial line with circular outer conductor having an anisotropic medium and the arrangement of line charges and contour points ($n = 36$).

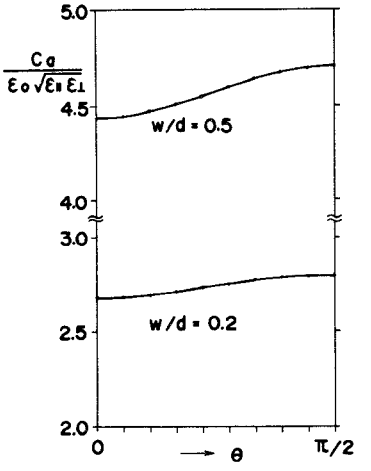

Fig. 9. Capacitances $Ca/\epsilon_0\sqrt{\epsilon_{\parallel}\epsilon_{\perp}}$ per unit length versus θ for the structure shown in Fig. 8 with sapphire dielectric.

TABLE III
COMPARISON OF THE CAPACITANCES C_0/ϵ_0 PER UNIT LENGTH FOR THE STRUCTURES WITH A CIRCULAR OUTER CONDUCTOR SHOWN IN FIG. 8

$\epsilon_{\parallel} = \epsilon_{\perp} = 1.0$		
$\frac{w}{d}$	C_0/ϵ_0	
	D:conformal mapping[2]	A:the method of this paper(n=36)
0.2	2.72899	2.72899
0.5	4.55873	4.55873

by a conformal mapping technique [2] as

$$C_0 = 4\epsilon_0 \frac{K'(k)}{K(k)} \quad k = \frac{1-(w/d)^2}{1+(w/d)^2}.$$

Table III shows very good agreement. Fig. 9 shows $Ca/\epsilon_0\sqrt{\epsilon_{\parallel}\epsilon_{\perp}}$ versus θ for the structures with zero-offset strip.

V. Conclusion

We have analytically presented the electric potential function in the anisotropic region. The potential function was applied to the charge simulation method. The numerical results of capacitances for two structures with sapphire dielectrics are also presented. This method is useful for the numerical analysis of the coaxial lines where the analytical formulas for the capacitance cannot be obtained.

The potential function (6) is applicable to the equivalent source method [25], but it is not described in this paper.

Acknowledgment

The authors would like to thank K. Kamata at Ibaraki Technical College for helpful discussions.

References

[1] M. L. Crawford, "Generation of standard EM fields using TEM transmission cells," *IEEE Trans. Electromagn. Compat.*, vol. EMC-16, pp. 189–195, Nov. 1974.

[2] W. Maguns and F. Oberhettinger, "Die berechnung des wellenwiderstandes," *Arch. Elektrotech.*, 37 Bund, Heft 8, pp. 380–390, 1943.

[3] G. M. Anderson, "The calculation of the capacitance of coaxial cylinders of rectangular cross-section," *AIEE Trans.*, vol. 69, pp. 728–731, Feb. 1950.

[4] S. B. Cohn, "Shielded coupled-strip transmission line," *IRE Trans. Microwave Theory Tech.*, vol. MTT-3, pp. 29–38, Oct. 1955.

[5] T. Chen, "Determination of the capacitance, inductance, and characteristic impedance of rectangular lines," *IRE Trans. Microwave Theory Tech.*, vol. MTT-8, pp. 510–519, Sept. 1960.

[6] J. C. Tippet and D. C. Chang, "Characteristic impedance of a rectangular coaxial line with offset inner conductor," *IEEE Trans. Microwave Theory Tech.*, vol. MTT-26, pp. 876–883, Nov. 1978.

[7] H. J. Riblet, "The characteristic impedance of a family of rectangular coaxial structures with off-centered strip inner conductors," *IEEE Trans. Microwave Theory Tech.*, vol. MTT-27, pp. 294–298, Apr. 1979.

[8] B. T. Szentkuti, "Simple analysis of anisotropic microstrip lines by a transform method," *Electron. Lett.*, vol. 12, pp. 672–673, Dec. 1976.

[9] E. Yamashita, K. Atsuki, and T. Mori, "Application of MIC formulas to a class of integrated-optics modulator analyses: A simple transformation," *IEEE Trans. Microwave Theory Tech.*, vol. MTT-25, pp. 146–150, Feb. 1977.

[10] S. Kusase and R. Terakado, "Mapping theory of two-dimensional anisotropic regions," *Proc. IEEE (Lett.)*, vol. 67, pp. 171–172, Jan. 1979.

[11] M. Kobayashi and R. Terakado, "New view on an anisotropic medium and its application to transformation form anisotropic to isotropic problems," *IEEE Trans. Microwave Theory Tech.*, vol. MTT-27, pp. 769–775, Sept. 1979.

[12] H. Shibata, S. Minakawa, and R. Terakado, "A method for equalizing the even- and odd-mode phase velocities of shielded coupled-strip line with an anisotropic medium," *Trans. Inst. Elect. Eng. Japan*, vol. 102-A, pp. 149–154, Mar. 1982 (in Japanese).

[13] H. Shibata, S. Minakawa, and R. Terakado, "Analysis of the shielded strip transmission line with an anisotropic medium," *IEEE Trans. Microwave Theory Tech.*, vol. MTT-30, pp. 1264–1267, Aug. 1982.

[14] T. Kohno and T. Takuma, *Numerical Calculation Method of Electric Field*. Tokyo: Corona-sha, 1980 (in Japanese).

[15] H. Shibata, S. Minakawa, M. Kobayashi, and R. Terakado, "Upper and lower bounds of the resistance value of two-dimensional anisotropic compound regions by supposing the potential distribution," *Trans. Inst. Elect. Eng. Japan*, vol. 98-A, pp. 494, Sept. 1978 (in Japanese).

[16] M. Panizo, A. Costellanos, and J. Rivas, "Finite-difference operators in inhomogeneous anisotropic media," *J. Appl. Phys.*, vol. 48, no. 3, pp. 1054–1057, Mar. 1977.

[17] H. Steinbigler, "Digitale berechnug elektrischer felder," *Elektotechnische Zeitschrift*, ETZ-A, Bund 90, pp. 663–666, 1969.

[18] H. Singer, H. Steinbigler, and P. Weiss, "A charge simulation method for the calculation of high voltage fields," *IEEE Trans. Power App. Syst.*, vol. PAS-93, pp. 1660–1668, 1974.

[19] S. Murashima, "Application of conformal mapping to charge simulation method," *Inst. Elect. Eng. Japan*, ED(PE)-79-3, pp. 21–30, 1979 (in Japanese).

[20] K. J. Binns and P. J. Lawrenson, *Analysis and Computation of Electric and Magnetic Field Problems*. New York: Pergamon, 1973, pp. 184–186.

[21] K. Tsuruta and R. Terakado, "Easy determination of the characteristic impedance of the coaxial system consisting of an inner regular polygon concentric with an outer circle," *IEEE Trans. Microwave Theory Tech.*, vol. MTT-28, pp. 147–149, Feb. 1980.

[22] S. Murashima, M. Kato, and E. Miyachika, "On the property of the error in the charge simulation method," *Trans. Inst. Elect. Eng. Japan*, vol. 98-A, pp. 39–46, Jan. 1978 (in Japanese).

[23] S. Murashima, H. Kondo, M. Yokoi, and H. Nieda, "Relation between the error of the charge simulation method and the location of charges," *Trans. Inst. Elect. Eng. Japan*, vol. 102-A, pp. 1–8, Jan. 1982 (in Japanese).

[24] J. Fontanella, C. Andeen, and D. Schuele, "Low-frequency dielectric constants of α-quartz, sapphire, MgF_2, and MgO," *J. Appl. Phys.*, vol. 45, pp. 2852–2854, July 1974.

[25] R. F. Harrington, K. Pontoppidan, P. Abrahamsen, and N. C. Albertsen, "Computation of Laplacian potentials by an equivalent-source method," *Proc. Inst. Elec. Eng.*, vol. 116, pp. 1715–1720, Oct. 1969.

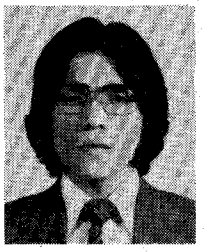

Hisashi Shibata was born in Takahagi, Ibaraki, Japan, on February 5, 1950. He received the B.E degree in electrical engineering from Ibaraki University, Ibaraki, Japan, in 1975.

He joined the Department of Electrical Engineering, Ibaraki Technical College, Ibaraki, Japan, in 1975, where he is now an Associate Professor. His current research interests are the analysis of electromagnetic fields in an anisotropic medium and the applications of the theory to the microwave devices.

Mr. Shibata is a member of the Institute of Electrical Engineers of Japan and the Institute of Electronics and Communication Engineers of Japan.

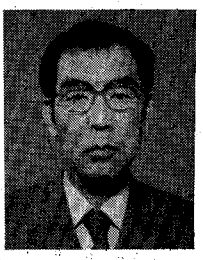

Shinya Minakawa was born in Hitachi, Ibaraki, Japan, on January 22, 1924. He graduated from the Taga Technical College, Ibaraki, Japan, in 1944.

In 1967 he joined the Department of Electrical Engineering, Ibaraki Technical College, Ibaraki, Japan, where he is now a Professor.

Mr. Minakawa is a member of the Institute of Electrical Engineers of Japan.

Ryuiti Terakado was born in Tokyo, Japan, on January 30, 1930. He graduated from the Taga Technical College, Ibaraki, Japan, in 1950. He received the D.E. degree from the Tokyo Institute of Technology, Tokyo, Japan, in 1975.

In 1960 he joined the Department of Electrical Engineering, Ibaraki University, where he is now a Professor. He is also a part-time lecturer at Ibaraki Technical College. His major research interests are two-dimensional fields and symmetry.

Dr. Terakado is a member of the Institute of Electrical Engineers, the Institute of Electronics and Communication Engineers, and the Society of Instrument and Control Engineers, all of Japan.